Pergamon

PII: S0306-4522(01)00188-9

www.elsevier.com/locate/neuroscience

Neuroscience Vol. 105, No. 2, pp. 413–429, 2001
© 2001 IBRO. Published by Elsevier Science Ltd
Printed in Great Britain. All rights reserved
0306-4522/01 $20.00+0.00

DEVELOPMENTAL CHANGES IN THE LOCALISATION OF THE mGluR1α SUBTYPE OF METABOTROPIC GLUTAMATE RECEPTORS IN PURKINJE CELLS

G. LÓPEZ-BENDITO,[a] R. SHIGEMOTO,[b] R. LUJÁN[c]* and J. M. JUIZ[c]

[a]Instituto de Neurociencias, Universidad Miguel Hernández, Campus de San Juan, Ctra. Valencia Km. 87, 03550 San Juan, Alicante, Spain

[b]Division of Cerebral Structure, National Institute for Physiological Sciences, Myodaiji, Okazaki 444-8585, CREST Japan Science and Technology Corporation, Japan

[c]Laboratorio de Neurohistología, Facultad de Medicina, Universidad Castilla-La Mancha, Campus de Albacete, 02071 Albacete, Spain

Abstract—The regulation of neurotransmitter receptors during synapse formation has been studied extensively at the neuromuscular junction, but little is known about the development of excitatory neurotransmitter receptors during synaptogenesis in central synapses. In this study we show qualitatively and quantitatively that a receptor undergoes changes in localisation on the surface of rat Purkinje cells during development in association with its excitatory synapses. The presence of mGluR1α at parallel and climbing fibre synapses on developing Purkinje cells was studied using high-resolution immunoelectron microscopy. Immunoreactivity for mGluR1α was detected from embryonic day 18 in Purkinje cells, and showed dramatic changes in its localisation with age. At early postnatal ages (P0 and P3), mGluR1α was found both in somata and stem dendrites but was not usually associated with synaptic contacts. At P7, mGluR1α became concentrated in somatic spines associated with climbing fibres and in the growing dendritic arborisation even before innervation by parallel fibres. During the second and third postnatal week, when spines and parallel fibre synapses were generated, mGluR1α became progressively concentrated in the molecular layer, particularly in the synaptic specialisations. As a result, during the fourth postnatal week, the pattern and level of mGluR1α expression became similar to the adult and mGluR1α appeared in high density in perisynaptic sites.

Our results indicate that mGluR1α is present in the developing Purkinje cells prior to their innervation by climbing and parallel fibres and demonstrate that this receptor undergoes a dynamic and specific regulation during postnatal development in association with the establishment of synaptic inputs to Purkinje cell. © 2001 IBRO. Published by Elsevier Science Ltd. All rights reserved.

Key words: neurotransmitter, immunocytochemistry, electron microscopy, cerebellum, rat.

Purkinje cells (PC) receive distinct types of excitatory inputs from parallel fibres (PFs), the ascending axons of granule cells, and climbing fibres (CFs) which originate in the inferior olive (Palay and Chan-Palay, 1974; Sotelo, 1978). In adults, PF synapses are established on spines of distal PC dendrites, whereas CF synapses are formed on spines along the proximal dendrites of PC (Palay and Chan-Palay, 1974; Sotelo, 1978; Ito, 1984). Both types of synapses develop during the first two postnatal weeks: functional CF synapses are present on PC somatic processes from postnatal day (P)2, whereas PF synapses begin forming at P7–P10 (Altman and Bayer, 1997). After PF and CF synapses are generated, they are dynamically modified during postnatal development, resulting in the elimination of redundant synapses.

The process of synapse elimination is crucial for cerebellar development, and has been well documented at the CF–PC synapse (Mariani and Changeux, 1980; Crépel et al., 1981). Each PC is innervated by several CFs during the first week after birth. A massive elimination of synapses then occurs, and the innervation of each PC by only one CF, found in the adult animal, is established at around P21 (Altman and Bayer, 1997). However, multiple innervation of the PC persists in adulthood in mutant animals lacking genes for ionotropic or metabotropic glutamate receptors (mGluRs) (Kashiwabuchi et al., 1995; Kano et al., 1997; Ichise et al., 2000).

mGluRs have modulatory functions on neuronal excitability and transmitter release and are involved in synaptic plasticity (Pin and Duvoisin, 1995). To date, eight different subtypes of mGluRs have been identified and termed mGluR1 through mGluR8. These different sub-

*Corresponding author. Tel.: +34-967-599200/2754; fax: +34-967-599202.

E-mail address: rlujan@med-ab.uclm.es (R. Luján).

Abbreviations: AMPA, α-amino-3-hydroxy-5-methyl-isoxazole-4-propionic acid; CF, climbing fibre; E, embryonic day; LTD, long-term depression; mGluR, metabotrophic glutamate receptor; NGS, normal goat serum; P, postnatal day; PB, phosphate buffer; PBS, phosphate-buffered saline; PC, Purkinje cell; PF, parallel fibre; PKC, protein kinase C; TB, Tris buffer; TBS, Tris-buffered saline.

types have been classified into three groups based on their sequence homology, transduction mechanisms and pharmacological profiles (Nakanishi, 1994; Pin and Duvoisin, 1995; Conn and Pin, 1997). Group I is activated most potently by quisqualate (Masu et al., 1991; Abe et al., 1992; Aramori and Nakanishi, 1992) and includes mGluR1 and mGluR5, which exist in a number of alternatively spliced forms (mGluR1α, β, c, d and mGluR5a, b). Group II includes mGluR2 and mGluR3, and Group III includes mGluR4, mGluR6, mGluR7 and mGluR8. Groups II and III are negatively coupled to adenyl cyclase and inhibit the forskolin-stimulated accumulation of cyclic AMP (Pin and Duvoisin, 1995; Conn and Pin, 1997).

The functions of mGluR1 have been extensively studied in the cerebellum because of its role in learning-related processes and its thoroughly characterised cytoarchitecture and synaptic circuitry (Aiba et al., 1994; Conquet et al., 1994; Ichise et al., 2000). mGluR1 is found at very high levels in PCs (Masu et al., 1991; Shigemoto et al., 1992). Immunoelectron microscopy has shown that, at least in adults, the mGluR1 protein is localised in spines of PC dendrites facing PF and CF terminals (Martin et al., 1992; Baude et al., 1993; Shigemoto et al., 1994; Luján et al., 1997; Nusser and Somogyi, 1997). A number of studies have shown that mGluR1 is found in the developing cerebellum (Shigemoto et al., 1992; Ryo et al., 1993) and there are indications suggesting an involvement of mGluR1 in the early formation of PC synapses (Kano et al., 1997; Levenes et al., 1997). Little is known, however, about how mGluRs become organised during synaptogenesis to respond efficiently to presynaptic glutamate release.

Information on the organisation and precise distribution of mGluRs at developing PC synapses is important in helping to determine what role these receptors may play in postnatal development. Therefore, in order to understand how mGluR distribution develops relative to specific excitatory inputs and becomes organised in adult PC synapses, we have applied high-resolution immunocytochemical techniques to reveal the subcellular localisation patterns of mGluR1α, the major splice variant of mGluR1 in the cerebellum (Casabona et al., 1997), during postnatal development of PCs.

EXPERIMENTAL PROCEDURES

Forty-three male Wistar rats from embryonic day (E)18 to adulthood, obtained from the Animal House Facilities of the University Miguel Hernandez, were used. The care and handling of the animal prior to and during the experimental procedures followed European Union regulations, and was approved and supervised by the University Animal House Facilities. We have minimised both the suffering and the number of animals used in this study.

For each developmental stage, the animals used were from different litters and were grouped as follows: E18 ($n=3$), day of birth = P0 ($n=4$), P3 ($n=4$), P5 ($n=4$), P7 ($n=4$), P10 ($n=4$), P12 ($n=4$), P15 ($n=4$), P21 ($n=4$), P30 ($n=4$) and P60 ($n=4$). All animals were deeply anaesthetised with an intraperitoneal injection of Rompun(xylazine; Bayer AG, Leverkussen, Germany)–Imalgene(ketamine; Merial Laboratories, Lyon, France) 1:1 (0.1 ml/kg body weight) and then the hearts were surgically exposed for perfusion fixation. First, the vascular system was flushed by circulating 0.9% saline with 0.1% sodium nitrite followed by transcardial perfusion of freshly prepared ice-cold fixative containing 4% paraformaldehyde, 0.05% glutaraldehyde and ~0.2% picric acid in 0.1 M phosphate buffer (PB, pH 7.2–7.4). After perfusion, brains were removed from the skull and immersed in the same fixative for 2 h at 4°C. Tissue blocks containing cerebellum were dissected and thoroughly washed in 0.1 M PB for several hours. Coronal 60-μm sections of cerebellum were cut with a vibratome and collected in 0.1 M PB.

Antibodies and controls

An affinity-purified polyclonal antibody against mGluR1α was made in rabbits. The characteristics and specificity of this antibody have been described elsewhere (Jaarsma et al., 1998).

As controls for method specificity, sections were incubated omitting the primary antibody. Other sections were incubated with 5% normal rabbit serum replacing the primary antibodies. Under these conditions, no immunoreactivity could be detected. Moreover, using a polyclonal rabbit antibody to Calretinin (Chemicon, Temecula, CA, USA), no plasma membrane labelling was observed with our pre-embedding or post-embedding methods, showing that the labelling found on the plasma membrane is due to the antibodies raised for the peptide sequence present in mGluR1α. As controls for the post-embedding method, we used polyclonal rabbit antibodies to α-amino-3-hydroxy-5-methyl-isoxazole-4-propionic acid (AMPA)-type glutamate receptor GluR2/3 (Chemicon). Under these conditions synaptic labelling was observed (data not shown), showing that mGluR1α is either absent from the main body of the synapse or present at concentrations below detection levels.

Immunocytochemistry

Pre-embedding immunoperoxidase method. Immunocytochemical reactions were carried out as described earlier (Baude et al., 1993; Luján et al., 1996). Free-floating sections were incubated in 10% normal goat serum (NGS) diluted in 50 mM Tris buffer (TB; pH 7.4) containing 0.9% NaCl (Tris-buffered saline, TBS), with or without 0.2% Triton X-100, for 1 h. Sections were then incubated for 48 h in an affinity-purified polyclonal antibody anti-mGluR1α at a final protein concentration of 1–2 μg/ml diluted in TBS containing 1% NGS. After washes in TBS, the sections were incubated for 2 h in biotinylated goat anti-rabbit IgG (Vector Laboratories, Burlingame, CA, USA) diluted 1:50 in TBS containing 1% NGS. They were then transferred into avidin–biotin-peroxidase complex (ABC kit, Vector Laboratories) diluted 1:100 for 2 h at room temperature. Peroxidase enzyme activity was revealed using 3,3′-diaminobenzidine tetrahydrochloride (0.05% in TB, pH 7.4) as chromogen and 0.01% H_2O_2 as substrate. Sections treated with Triton X-100 were used exclusively for light microscopy.

Pre-embedding immunogold method. Sections for the pre-embedding immunogold method were incubated together with those used for peroxidase reaction up to the secondary antibody stage. They were then incubated for 3 h in goat anti-rabbit IgG coupled to 1.4 nm gold (Nanoprobes Inc., Stony Brook, NY, USA) diluted 1:100 in TBS containing 1% NGS. After several washes in phosphate-buffered saline (PBS), the sections were postfixed in 1% glutaraldehyde dissolved in the same buffer for 10 min. They were washed in double distilled water, followed by silver enhancement of the gold particles with an HQ Silver kit (Nanoprobes Inc., Stony Brook, NY, USA).

The peroxidase-reacted sections and the gold–silver-labelled sections were processed for electron microscopy. This included treatment with OsO_4 (1% in 0.1 M PB), block-staining with uranyl acetate, dehydration in graded series of ethanol and flat-embedding on glass slides in Durcupan (Fluka, Chemie AG, Germany) resin.

Post-embedding immunogold method. The procedure was similar to that utilised by Luján and co-workers (1996). Briefly, ultrathin sections 60–80-nm thick from Lowicryl-embedded blocks of cerebellum (Baude et al., 1993; Luján et al., 1996) were picked up on coated nickel grids and incubated for 45 min on drops of a blocking solution consisting of 20% NGS in 0.05 M TBS, containing 0.9% NaCl and 0.03% Triton X-100. The grids were transferred to solutions of mGluR1α antibody at a concentration of 10 μg/ml in 0.05 M TBS with 2% NGS, containing 0.9% NaCl and 0.03% Triton X-100. Incubation in the primary antibody proceeded overnight at room temperature. After washing, the grids were incubated for 2 h on drops of goat anti-rabbit IgG conjugated to 10 or 15-nm colloidal gold particles (Nanoprobes) diluted 1:80 in 2% normal human serum and 0.5% polyethylene glycol in 0.05 M TBS containing 0.9% NaCl. The grids were then washed in TBS for 30 min and counterstained for electron microscopy with saturated aqueous uranyl acetate followed by lead citrate.

Quantification of immunoreactivity during postnatal development following pre-embedding immunogold labelling

The procedure was similar to that used earlier (Luján et al., 1996, 1997). Two samples were taken from the cerebellar molecular layer from two blocks of two animals at each age (P10, P15, P21 and P60). Electron microscopic sections were cut from the surface of 60-μm thick sections, as immunoreactivity decreases with depth. Randomly selected areas were photographed and printed to a final magnification of 45 000× and measurements covered a total section area of ~1000 μm^2 at each age. All dendritic spines establishing synapses with PFs were counted and assessed for the presence of immunoparticles; somatic or dendritic spines making synapses with CFs were not included in the present study, as they had complex morphologies. Only spine heads were analysed since spine necks are rarely connected to spine heads in single sections. The length of the synaptic membrane specialisation and the extrasynaptic membrane from all immunopositive spines at each age was measured using a digitising tablet and MAC-STEREOLOGY software (Ranforly MicroSystems, UK). The extrasynaptic spine membrane was divided into 60-nm bins. The distance between the centre of the immunoparticles and the closest edge of the postsynaptic density was measured along the spine membrane.

For the estimation of the relative proportion of receptor immunoreactivity at different positions in spines at each age, the area of membrane as a function of distance from the synaptic junction was estimated by approximating spine heads with spheres and spine necks with cylinders (Luján et al., 1997). Finally, the position of each immunoparticle within the sections with respect to the edge of the postsynaptic density was measured.

In order to compare the level of immunoreactivity for mGluR1α between material processed by the pre-embedding procedure that involves osmium fixation before dehydration and the post-embedding procedure lacking osmium fixation, the total number of immunoparticles along the plasma membrane were counted within individual dendritic spines establishing synapses with PFs as described above. For the post-embedding method, two samples were taken from two blocks of two animals at each postnatal age, and measurements were obtained from photographs at a final magnification of 40 000×. For comparisons, data were expressed as the number of immunoparticles per dendritic spine.

For the estimation of the background level in our incubations using the post-embedding technique, quantification was carried out from four sections for each one of the three rats at each postnatal age (P5, P10 and P60), and for each rat a field of 149 μm^2 of the cerebellar molecular layer was randomly photographed. Immunoparticles were counted within individual dendritic spines and the length of their plasma membrane was also measured on each ultrathin section from photographs at a final magnification of 38 000×. These data were expressed as density of immunoparticles per μm^2 of the dendritic spine plasma membrane.

Statistical analyses

The Kolmogorov–Smirnov non-parametric test was used to examine whether samples taken for each postnatal age were from a homogeneous population. All remaining statistical comparisons were done using the Mann–Whitney test. The differences were considered significant at the level of $P < 0.05$. Data are presented as mean ± S.D.

RESULTS

To establish correlation between the distribution of glutamate receptors and the formation of the glutamatergic neurotransmission system, we studied the expression pattern and subcellular localisation of mGluR1α during PC development. Immunocytochemistry revealed that mGluR1α is expressed early in this cell type (Fig. 1), though labelling intensity was irregular among PCs in different folia (see for instance Fig. 1C), suggesting variations in the rate of maturation of PCs. Therefore, the descriptions that follow are based on sections taken from the same region of the cerebellum (folia III–V) to eliminate variations due to regional differences.

Distribution of mGluR1α at the light microscopic level

Immunoreactivity for mGluR1α was seen in the PC layer on E18, the earliest age we studied (Fig. 1A). The intensity of labelling in developing PCs was characterised by a progressive increase with age until P21, when adult levels were reached (Fig. 1).

During the first week of development, intense mGluR1α immunoreactivity was observed in the undifferentiated PC layer (Figs. 1B–D and 2A). Immunolabelling was confined mainly to PC cell bodies and their developing stem dendrites (see for instance Fig. 2A).

At P7, mGluR1α immunoreactivity extended throughout the PC dendritic arbor emerging from each soma, including small branches (Fig. 2B, C). Dendritic arborisations became apparent in the molecular layer as PC dendrites grew towards the surface of the cerebellar lobe (Fig. 2B, C). At higher magnifications, it was evident that immunolabelling was particularly strong in PC somatic spines and some spines on the growing dendritic tree (Fig. 2C). Compared to the prominent immunoreactivity in PCs, only weak staining was seen in the internal granular layer, while the developing external granular layer showed no detectable immunolabelling (Fig. 2B). This indicates that granule cells do not express detectable amounts of mGluR1α proteins until they have migrated to the internal granular layer. In the internal granular layer, intermediate-size stained neurones, possibly Golgi cells, were scattered among the general population of granule cells (Fig. 2B).

Throughout the second postnatal week, immunoreactivity for mGluR1α increased continuously and outlined newly developing dendritic branches in the molecular layer (Fig. 2D, E). At P10, strong mGluR1α immunoreactivity was confined to PC bodies and their dendrites in the molecular layer, with much less intense immunoreactivity in granule cells (Fig. 2D). A higher number of

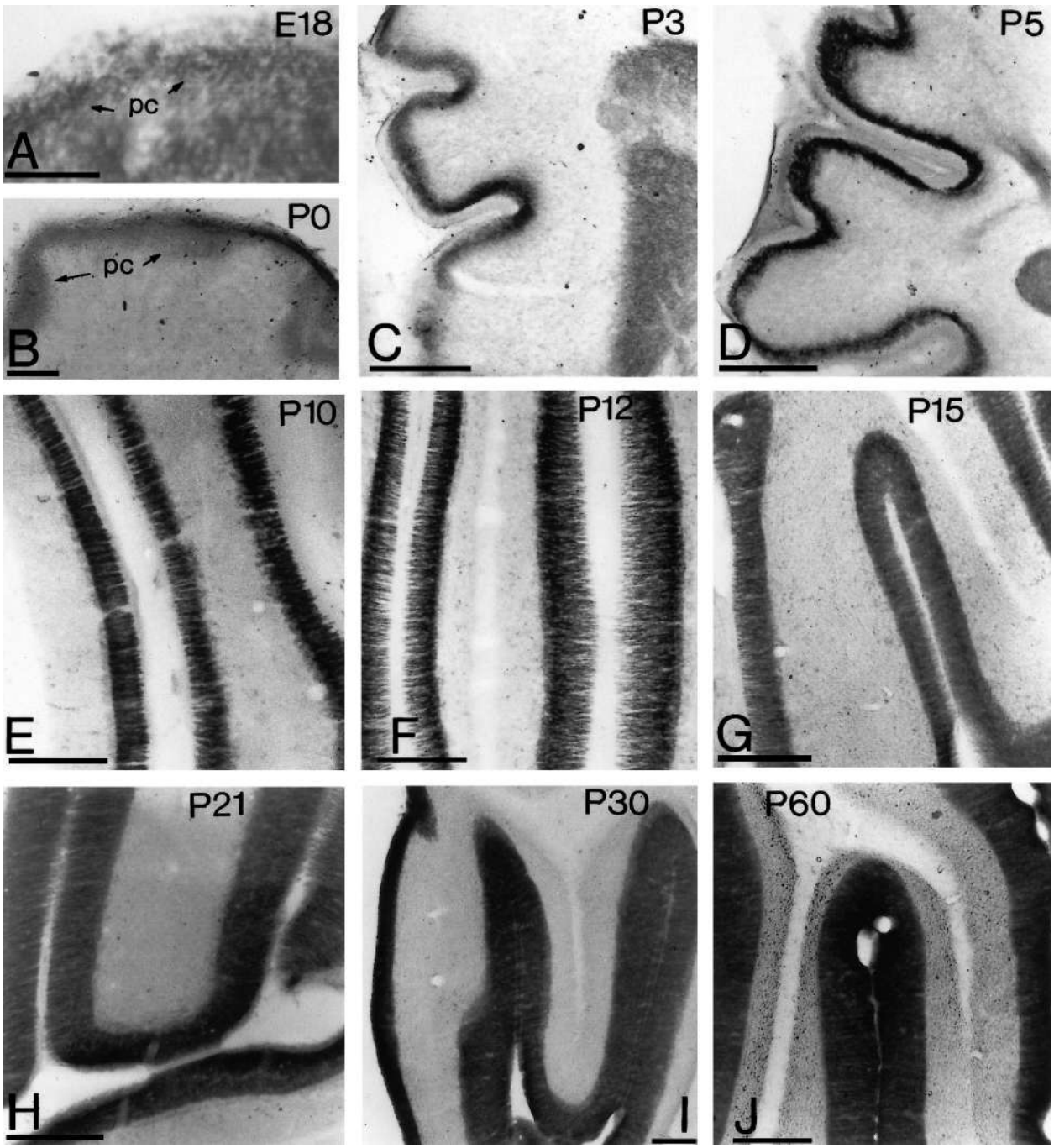


Fig. 1. Coronal sections of developing rat cerebella immunolabelled for mGluR1α. Immunoreactivity was detected at E18 in the PC layer and gradually increased with age until P21, when the adult pattern was reached. Scale bars: A–J, 100 μm.

somatic spines was intensely labelled at this age. Immunolabelled somatic spines were large and surrounded the entire PC soma (Fig. 2E). At P12, the receptor remained in PC somata and spread progressively throughout the entire dendritic arbor (Fig. 2F). At the same time, somatic spines were disappearing from the basal portion of the cell bodies remaining confined to the upper part of the PC somata (Fig. 2G, H).

During the third week of development, the molecular layer was still expanding. Immunoreactivity for mGluR1α was weaker in PC somata and stronger in the entire dendritic arborisation compared to previous postnatal ages (Fig. 2I). At P15, PC somatic spines completely disappeared and only faint mGluR1α immunoreactivity outlined PC cell bodies (Fig. 2I).

At P21, immunoreactivity for mGluR1α was still concentrated in the molecular layer (Fig. 2J). Dendritic arborisation was more compact and immunolabelling was strong and punctate (Fig. 2J). At this age, the pattern and intensity of mGluR1α expression closely matched that of the adult, which was characterised by very strong immunolabelling in the molecular layer and

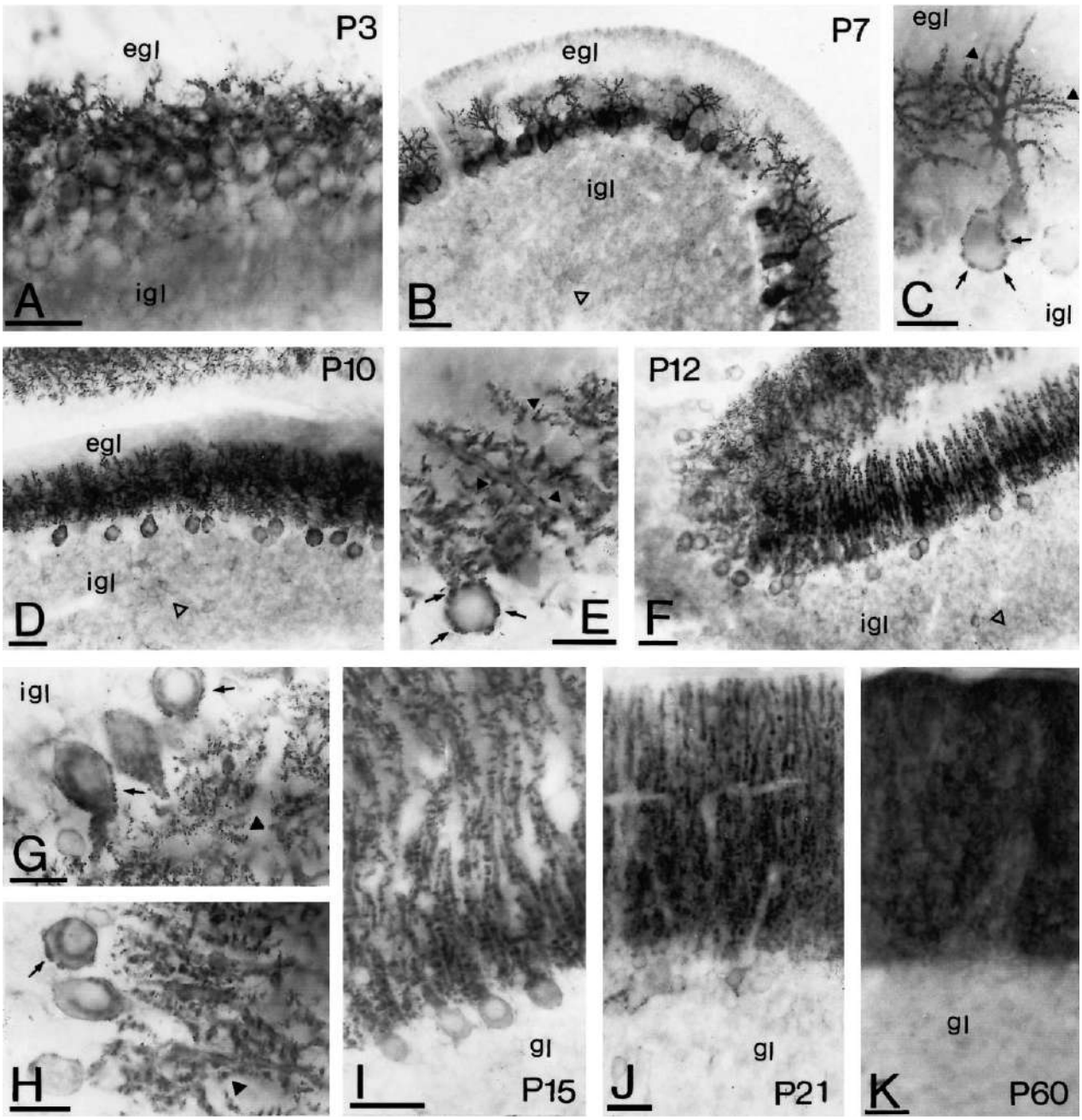


Fig. 2. Light microscopy distribution of mGluR1α in postnatal cerebellum. (A) At P3, strong immunolabelling for mGluR1α was visible in PC bodies and stem dendrites. (B, C) With ongoing development (P7) PC bodies and growing dendritic trees were immunolabelled. Immunoreactivity for mGluR1α was concentrated in somata (arrows in C) and in spine-like structures in the molecular layer (closed triangles). (D, E) At P10, mGluR1α was concentrated in the molecular layer (closed triangles), but still very prominent in somatic spines (arrows). (F–H) At P12, mGluR1α disappeared from the lower parts of the PC somata, being confined to the upper portions only (arrows). (I) At P15, mGluR1α disappeared completely from the somata. (J) At P21, immunoreactivity for mGluR1α resembled that of the adult (K). During development, granule cells were weakly immunolabelled and medium-size neurones (open arrowheads) were also observed. egl, external granular layer; igl, internal granular layer; gl, granule cell layer. Scale bars: A, B, D, F, I, J, K, 100 μm; C, E, G, H, 30 μm.

faintly stained PC somata (Fig. 2K). The molecular layer showed intense labelling, as compared to the much weaker labelling found in the granule cell layer (Fig. 2K).

Distribution of mGluR1α at the electron microscopic level

To establish the precise subcellular distribution of mGluR1α during development, the receptor was studied with pre-embedding immunoperoxidase and with pre- and post-embedding immunogold methods at the electron microscopic level. The three different techniques provided complementary information (Luján et al., 1996). The peroxidase reaction end-product for mGluR1α diffused from the plasma membrane, filling

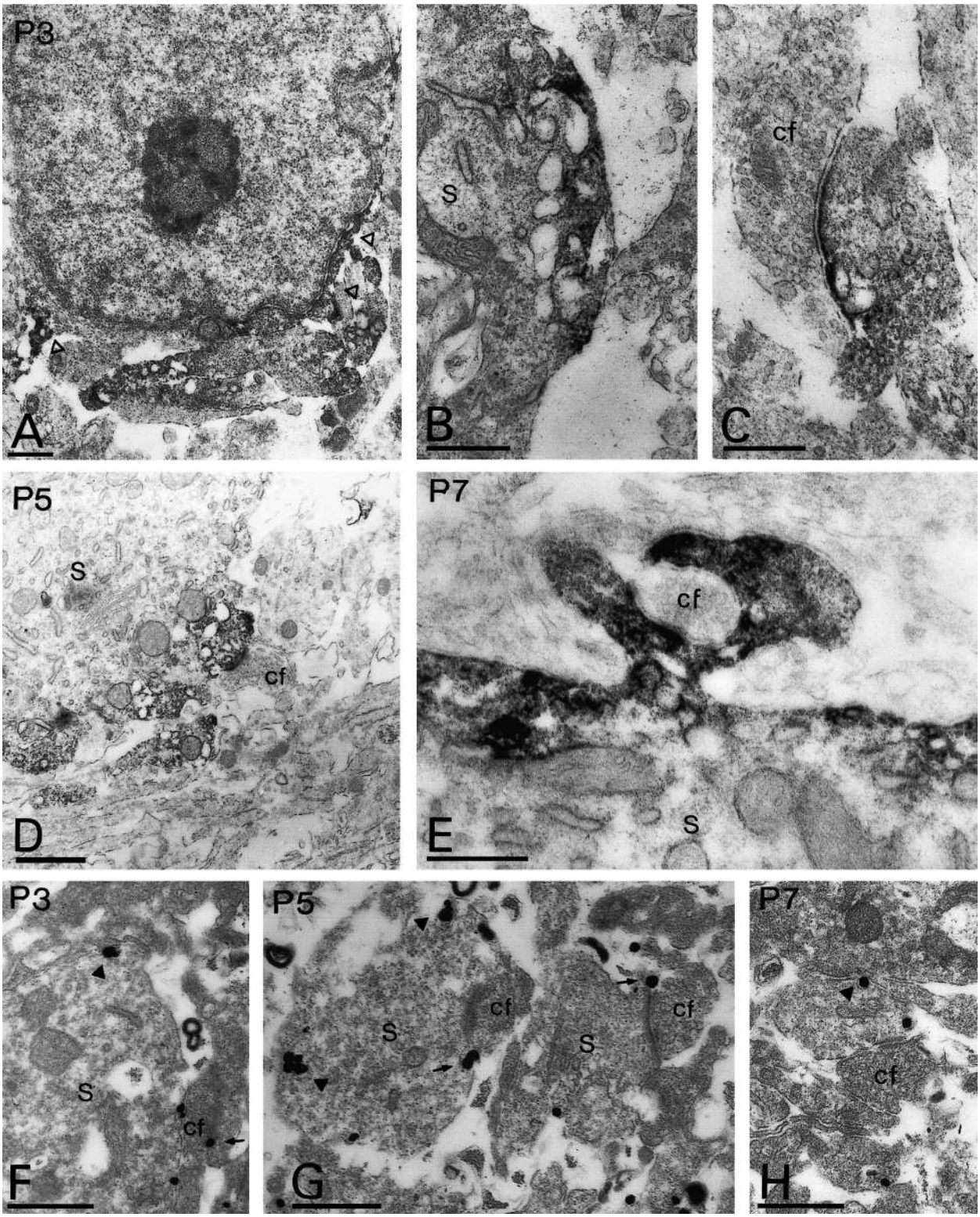


Fig. 3. Electron micrographs of the cerebellar cortex showing immunoreactivity for mGluR1α detected by pre-embedding immunoperoxidase (A–E) and immunogold methods (F–H). (A–C) At P3, immunoreactivity for mGluR1α was uniformly distributed in PCs (e.g. open triangles) or in patches associated with the membrane of the cell surface before the establishment of synaptic contacts. Some CF synapses were already detected at this age and immunoreactivity was concentrated at the postsynaptic level. (D) At P5, immunoreactivity for mGluR1α concentrated close to the somatic (S) plasma membrane facing CFs. (E) At P7, mGluR1α was localised in somatic spines embracing and establishing synapses with CFs. (F–H) Immunoparticles were located at the extrasynaptic (arrowheads) and perisynaptic (arrows) membranes of PC somata (S) or dendrites. Scale bars: A–C, E–H, 0.5 μm; D, 1 μm.

immunopositive somatic and/or dendritic profiles and also covering the postsynaptic membrane specialisations (e.g. Fig. 3C, D). The use of this sensitive method enabled us to establish the immunoreactivity of a particular structure, but its diffusion prevented determination of the precise location of the receptors. The pre-embedding immunogold method overcomes this technical limitation by resulting in a non-diffusible marker and electron-dense deposits along cell membranes. However, the density of immunoparticles decreases gradually with depth of the incubated section due to the limited penetration of immunoreagents. Regarding post-embedding reactions, all immunoreagents have direct access to the molecules present at the surface of the ultrathin section along the whole cut length of membranes. Therefore, this is the only method that provides accurate localisation of synaptic receptors. However, the labelling obtained with this technique is weaker than that of equivalent sites observed with the pre-embedding method.

At P0, immunoperoxidase reaction product was diffusely distributed within PC somata and most of the labelling was localised close to the plasma membrane. At P3–P5, labelling was mainly restricted to PC somata (Fig. 3A) and stem dendrites. In PC somata, immunoperoxidase reaction product was associated with intracellular membranes, and was distributed close to the plasma membrane (Fig. 3A, B), as found at every developmental age studied. Immunolabelling for mGluR1α in the developing somata was found in membrane patches at the cell surface, often associated with adjacent axonal processes and the establishment of immature synaptic contacts (Fig. 3B). Very few presynaptic terminals identifiable as CFs (Altman and Bayer, 1997) were detected establishing synapses on the PC somata at this age (e.g.

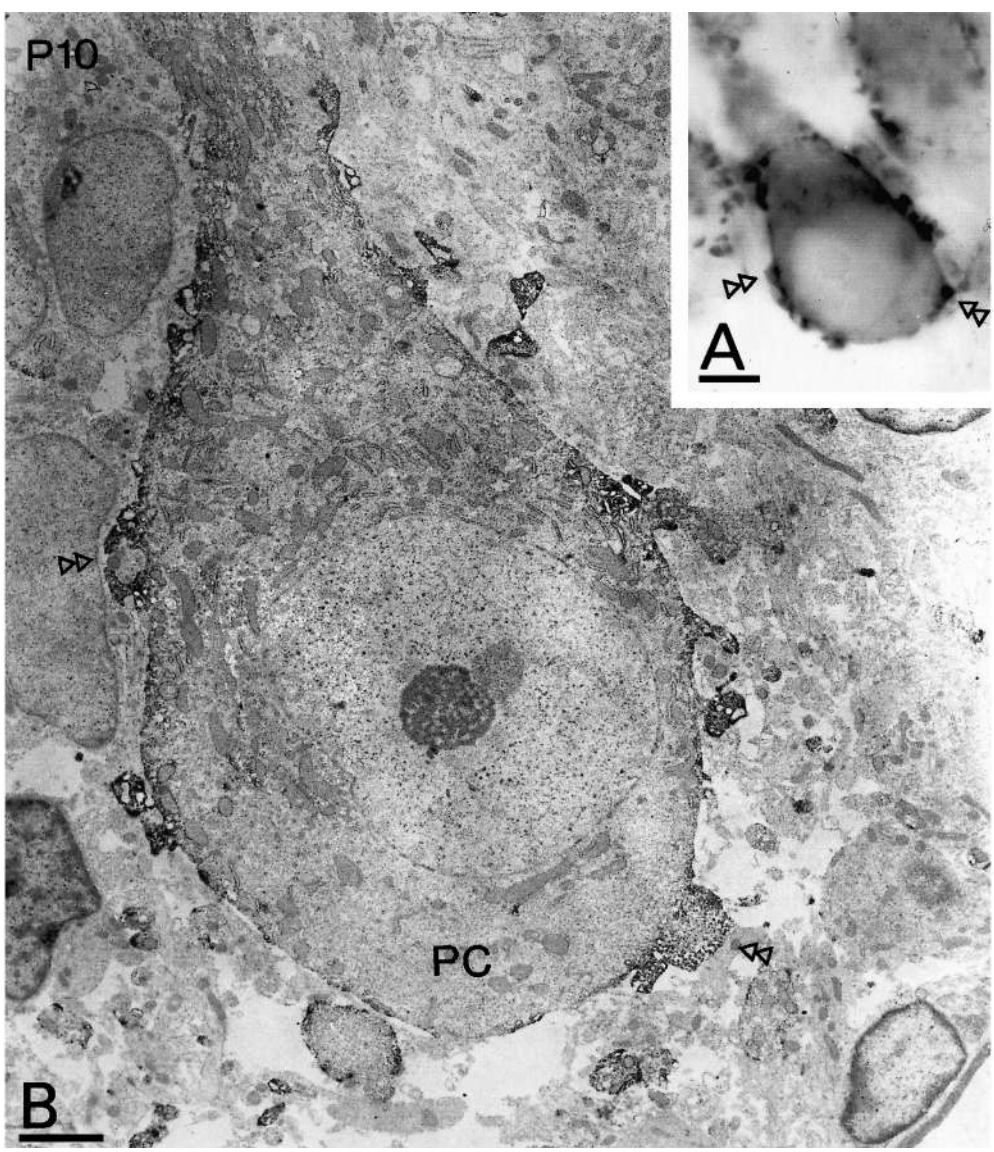


Fig. 4. Light and electron micrographs of the same mGluR1α-immunoreactive PC labelled by the pre-embedding immunoperoxidase method. (A, B) The immunolabelling for mGluR1α around the soma detected using light microscopy corresponded to somatic spines (double open triangles) when observed with the electron microscope (double open triangles). Scale bars: A, B, 2 μm.

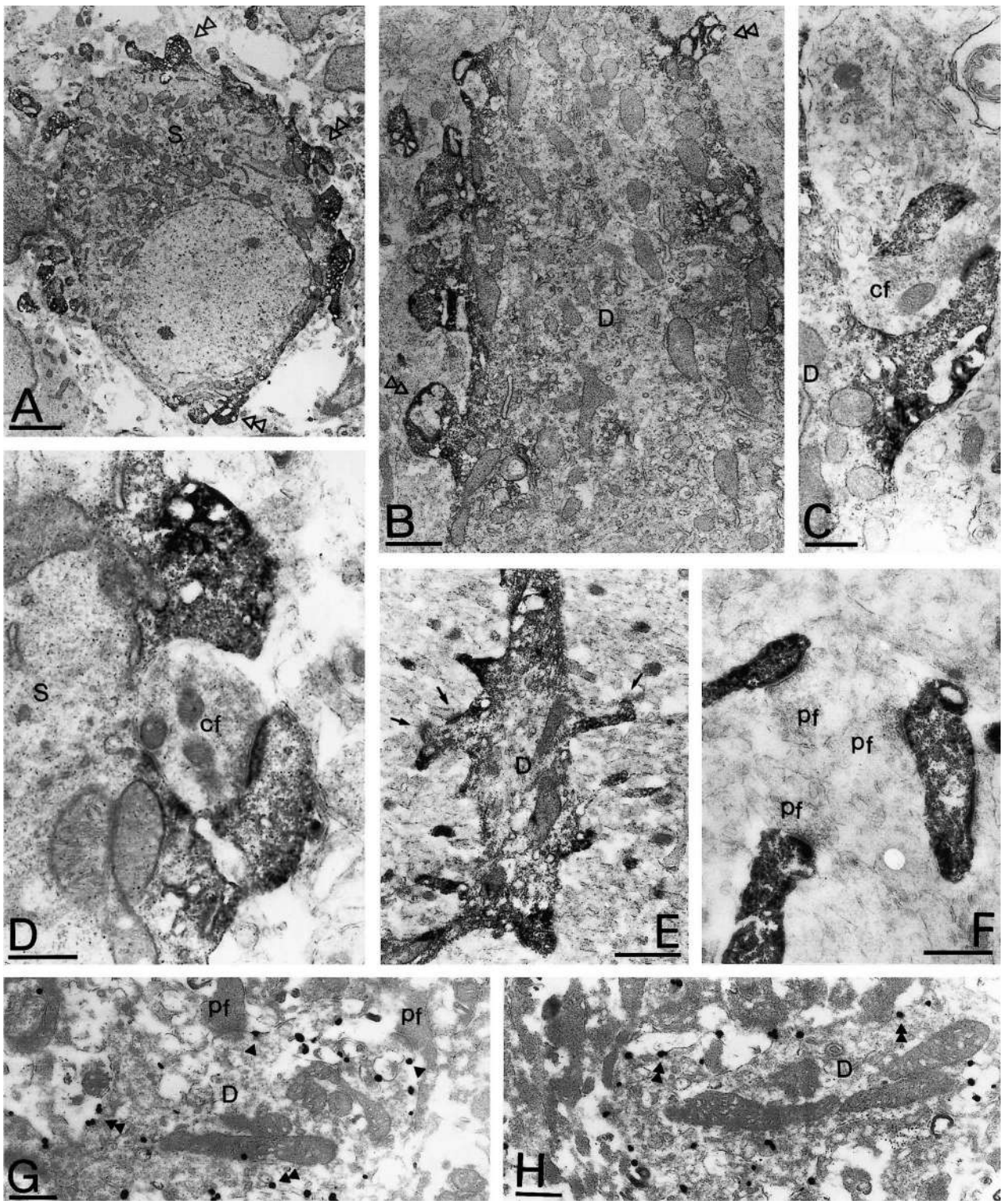


Fig. 5. Immunoreactivity for mGluR1α at P10 in PCs revealed by pre-embedding immunoperoxidase and immunogold methods. (A–D) Immunolabelling was concentrated in somatic spines (A, C) and lateral processes of the main dendritic shaft (B, C) (double open triangles in A and B). These processes embraced CFs and made synaptic contacts with them. (E, F) In the molecular layer, mGluR1α was detected in morphologically immature dendritic spines establishing synapses with PF. (G, H) Immunoparticles were located at the extrasynaptic (double closed triangles) and perisynaptic (closed triangles) membranes of PC somata or dendrites (D). Scale bars: A, 2 μm; B, E, G, 1 μm; C, D, F, H, 0.5 μm.

Fig. 3C, D). Postsynaptic densities at the synaptic contacts were asymmetrical (Fig. 3C, D). Nuclei were always devoid of reaction product (e.g. Fig. 3A) and no labelling was visualised in either presynaptic axon terminals or glial cells. Symmetrical synapses on mGluR1α immunolabelled profiles were not observed at this stage of development. Using the pre-embedding immunogold method, immunoparticles were located on plasma membranes and, less frequently, scattered in the cytoplasm (Fig. 3F, G). Membrane-associated immunoparticles were located in perisynaptic positions or associated with the extrasynaptic plasma membrane (Fig. 3F, G).

At P7, CF terminals were numerous and immunoreactivity for mGluR1α was concentrated in somatic spines emerging from the cell body (Fig. 3E). Synapses formed by CFs with PCs were more frequently found at P7 than

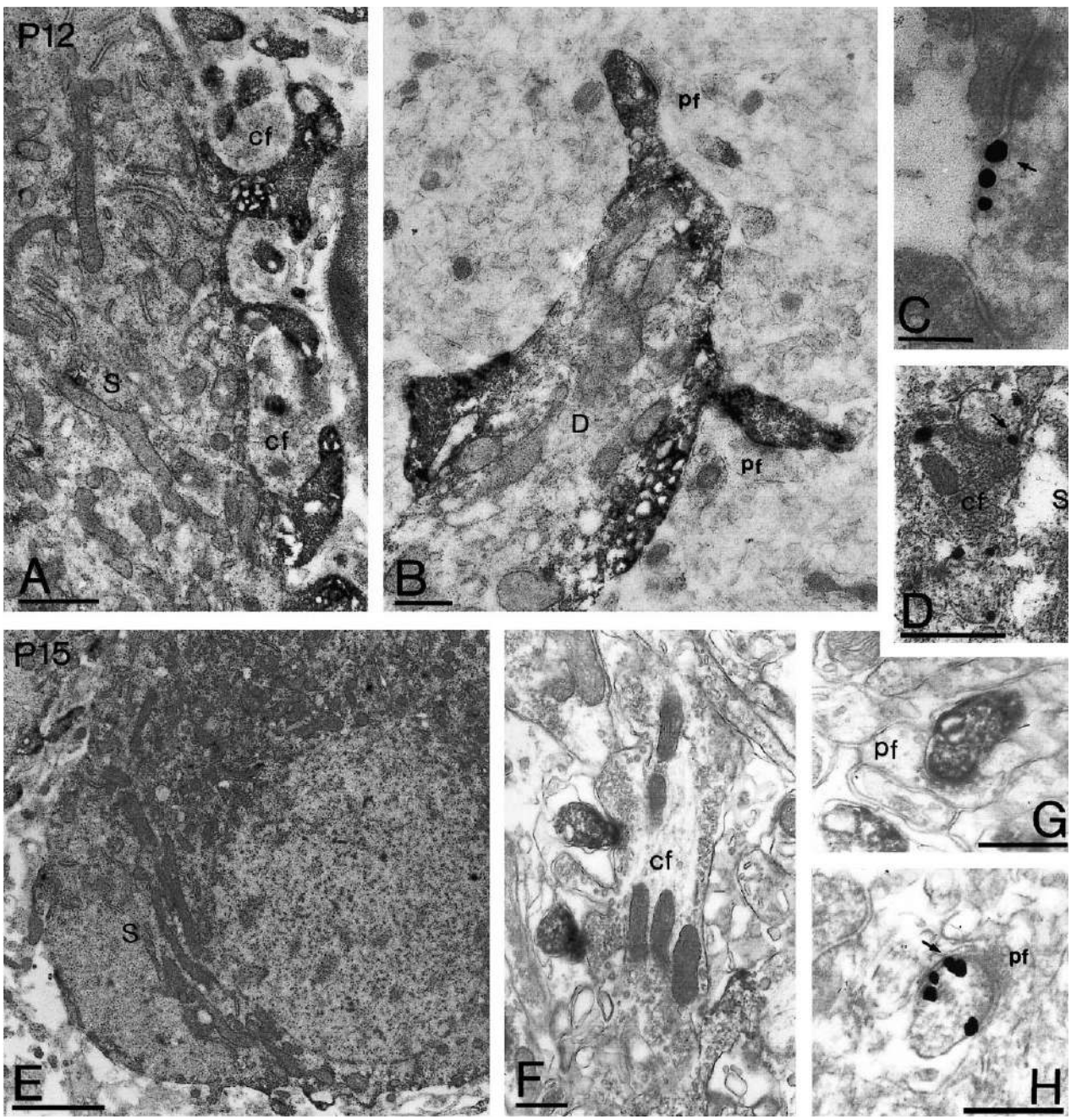


Fig. 6. Electron micrographs of the cerebellar cortex showing immunoreactivity for mGluR1α revealed by pre-embedding immunoperoxidase and immunogold methods at P12 and P15. (A–D) At P12, immunoreactivity for mGluR1α was detected in somatic spines facing CFs located in the upper portions of PC somata (S). In the molecular layer, immunoreactivity became progressively concentrated in dendritic spines facing PFs. Immunoparticles were restricted to the plasma membrane, always outside the postsynaptic density. (E–H) At P15, somatic spines disappeared completely from the somata and CFs were found establishing synapses with dendrites and dendritic spines labelled for mGluR1α in the molecular layer. mGluR1α was very abundant in spines establishing synapses with mature PFs. Immunoparticles were concentrated in the plasma membrane of spines facing PFs or CFs. Scale bars: A, 1 μm; E, 2 μm; B, D, F–H, 0.5 μm; C, 0.2 μm.

at earlier ages, but still had immature morphological features. In the developing molecular layer, immunolabelling for mGluR1α was found both in dendritic membrane patches and immature dendritic spines prior to the arrival of axon terminals and the establishment of PF synaptic contacts. Immunoparticles were located in perisynaptic positions or associated with the extrasynaptic plasma membrane (Fig. 3H).

During the second postnatal week, the strong immunoreactivity for mGluR1α associated with the somata of PCs identified by light microscopy, was mainly due to the staining of somatic spines embracing CFs (e.g. Fig. 4). Immunoperoxidase reaction product was present along the somatic plasma membrane associated with CFs (Figs. 4 and 5A–D) and, at P12, in somatic spines in the upper portion of the cell body (Fig. 6A). The cytoplasm and nucleus were generally devoid of any labelling, with the exception of some intracellular membranes showing small patches of peroxidase reaction product (Figs. 4, 5A and 6E). The emerging main dendrite also contained spine-like lateral processes establishing synapses with CFs which had features similar to those observed close to the cell body (Fig. 5A, B). PC somatic spines formed many synaptic contacts and had the appearance of irregular, spine-like structures usually lacking organelles (Fig. 5C, D), very often embracing CF terminals (Figs. 3E and 5A–D). Synaptic contacts were established at different positions on the somatic spines.

In the molecular layer, immunoreactivity for mGluR1α originated from the staining of PC dendritic spines (Fig. 5E, F). Labelled dendritic spines were seen unattached to axon terminals or, more frequently, establishing synapses with unlabelled terminals identified as PFs

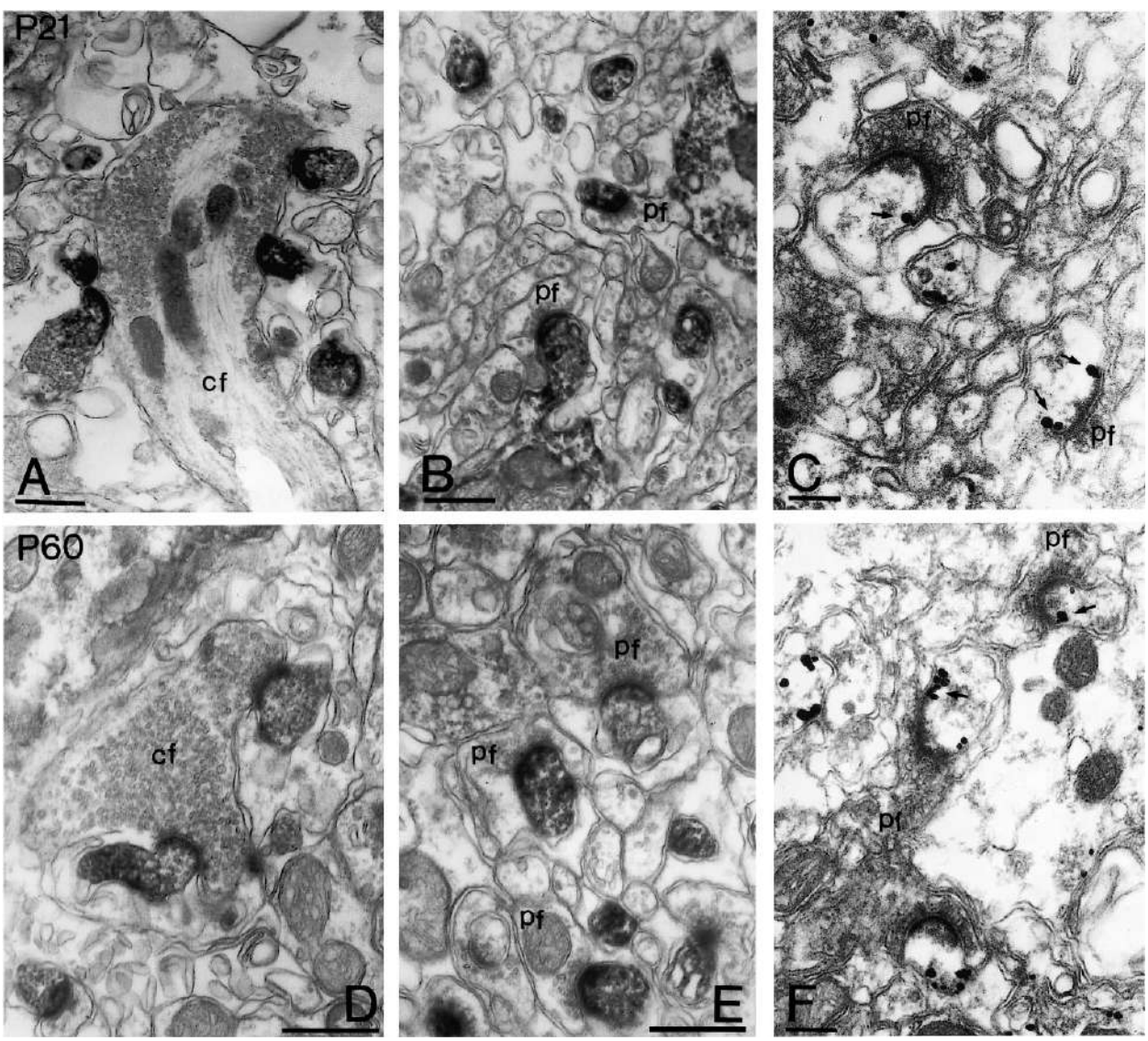


Fig. 7. Electron micrographs of the cerebellar cortex showing immunoreactivity for mGluR1α as revealed by pre-embedding immunoperoxidase and immunogold methods at P21 and P60. (A–F) The adult pattern of mGluR1α distribution was achieved by P21. Immunoreactivity for mGluR1α was localised in immunolabelled spines establishing synapses with PFs and CFs. Immunoparticles became progressively concentrated in perisynaptic sites (arrows), and were also present in extrasynaptic sites. Scale bars: A, B, D, E, 0.5 μm; C, F, 0.2 μm.

(Figs. 5E, F, and 6B for P12). The synaptic specialisation of these asymmetrical synapses was covered with immunoperoxidase reaction product (e.g. Figs. 5F and 6B). At P10, PF–PC synapses had immature morphological features, including small terminal swellings with few synaptic vesicles, small synaptic contacts and they were incompletely surrounded by Bergmann glial processes (Fig. 5F).

In immunogold-labelled sections using the pre-embedding technique, particles were widely distributed in somatic spines, dendritic profiles and dendritic spines (Fig. 5G, H). Immunoparticles were mainly associated with the plasma membrane (Fig. 5G, H) at extrasynaptic sites and at perisynaptic membrane sites (Figs. 5G, H and 6C, D) adjacent to the postsynaptic density of CF–PC and PF–PC synapses.

During the third postnatal week, PC somatic spines disappeared (Fig. 6E) and immunoreactivity for mGluR1α was located at non-synaptic sites. In the molecular layer, immunolabelling was mainly found in dendritic spines facing PFs and CFs (Fig. 6F–H).

At P21, the subcellular localisation of mGluR1α already resembled that of the adult animal (Fig. 7). Labelling for mGluR1α was restricted to dendritic spines attached to unlabelled presynaptic terminals (Fig. 7). Labelled PF–PC dendritic spines increased (Fig. 7B, E) and CF–PC dendrites immunoreactive for mGluR1α were also more easily detected in the molecular layer (Fig. 7A, D). Immunoparticles were present in dendritic spines and concentrated at perisynaptic sites (Fig. 7C, F). Axonal projections, glial processes and symmetrical synapses lacked mGluR1α immunoreactivity at all stages.

Finally, to provide direct evidence that the strong mGluR1α labelling associated with CFs and PFs was due to the localisation of the receptor at the perisynaptic and extrasynaptic level, but not at the synaptic level, we used a post-embedding immunogold technique. Immunolabelling for mGluR1α was examined at three different ages (P5, Fig. 8A; P10, Fig. 8B; and P60, Fig. 8C) representative of the developmental changes found with the pre-embedding method. At the three ages studied, immunoparticles were excluded from synaptic membranes (Fig. 8). Instead, gold particles associated with CFs and PFs were preferentially located at perisynaptic and extrasynaptic membrane areas (Fig. 8).

The labelling obtained using the post-embedding immunogold technique was always weaker than that observed using the pre-embedding method in both adult and developing animals. At P5, the difference between techniques in the absolute number of immunoparticles per spine in individual sections was large (post-embedding reaction, 1.52 ± 0.49 particles/spine; pre-embedding reaction, 2.97 ± 1.09 particles/spine). At P10, that difference was: post-embedding reaction, 1.91 ± 0.97 particles/spine; pre-embedding reaction 3.16 ± 1.34 particles/spine. At P60, the difference was reduced (post-embedding reaction, 2.11 ± 1.07 particles/spine; pre-embedding reaction, 3.54 ± 1.69 particles/spine). However, no difference in distribution of immu-

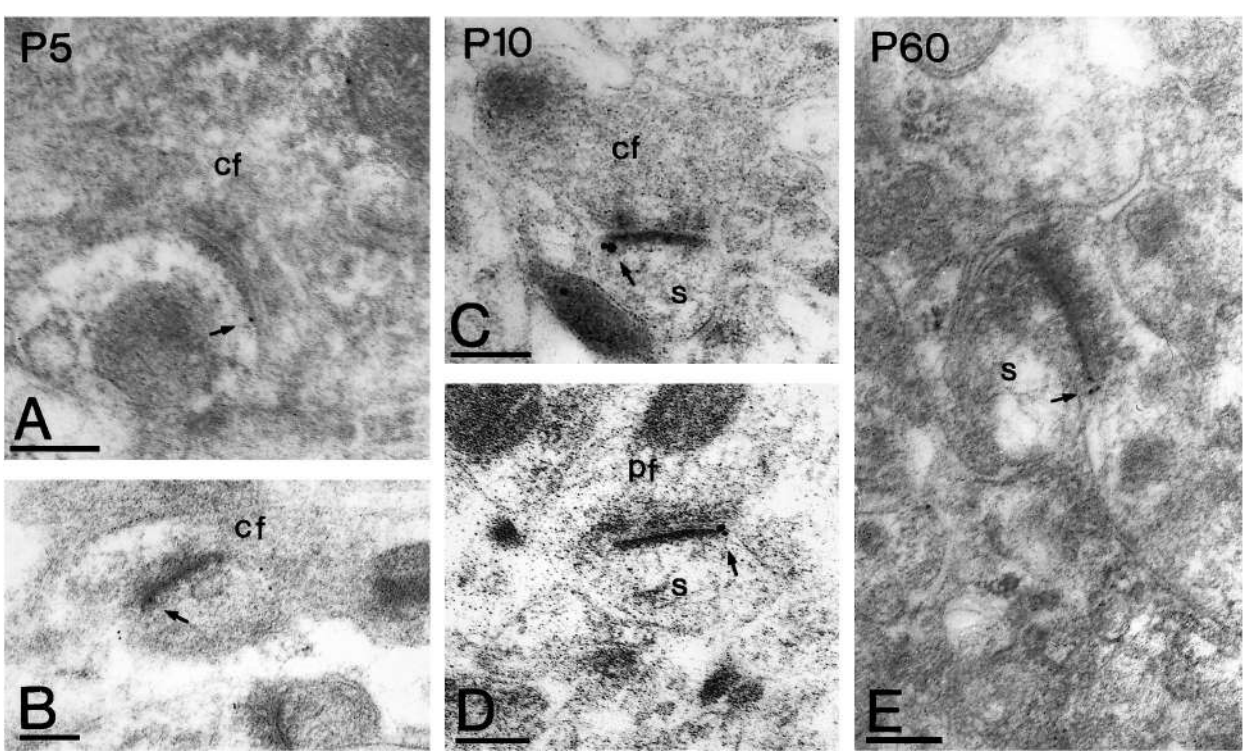


Fig. 8. Electron micrographs of the cerebellar cortex showing immunoreactivity for mGluR1α as detected by a post-embedding immunogold method at P5 (A,B), P10 (C,D) and P60 (E). Gold particles were never detected in the anatomically defined synaptic junctions at any age, but rather at perisynaptic (arrows) or extrasynaptic sites only. cf, climbing fibres; pf, parallel fibres; s, somata. Scale bars: A–E, 0.2 μm.

noparticles was detected between the two methods, ($P < 0.069$), confirming that the quantitative results obtained with the pre-embedding method are not biased by the differential accessibility of the epitopes (see next Section).

In addition, to determine whether the relatively low intensity of labelling using post-embedding reactions was specific or due to background, we carried out quantitative studies on control incubations. The density of particles (mean ± S.D., $n = 3$ rats for each age) when the primary antibody was omitted, was negligible: at P5, 0.129 ± 0.011 immunoparticles/μm^2; at P10, 0.132 ± 0.013 immunoparticles/μm^2; and at P60, 0.139 ± 0.016 immunoparticles/μm^2. This indicates that the low intensity of labelling detected with our post-embedding immunogold method is due to the specific antibody and, therefore, that mGluR1α is found mainly outside synaptic sites.

Quantitative comparison of the location of mGluR1α during postnatal development following pre-embedding immunogold labelling

To establish the relative densities of mGluR1α in relation to glutamate release sites (PF synapses) during postnatal development, measurements were taken from single and serial EM sections. The densities of mGluR1α relative to CF synapses have not been included in the present study because of the complex and irregular morphology of the somatic spines.

The position of immunoparticles (P10, $n = 317$; P15, $n = 321$; P21, $n = 329$; P60, $n = 314$) was measured from the closest edge of the synaptic specialisation. Data are displayed as frequency of particles in arbitrarily chosen 60-nm wide segments of the membrane of dendritic spines, starting at the edge of the synaptic membrane specialisation. Two samples, one from each of two ani-

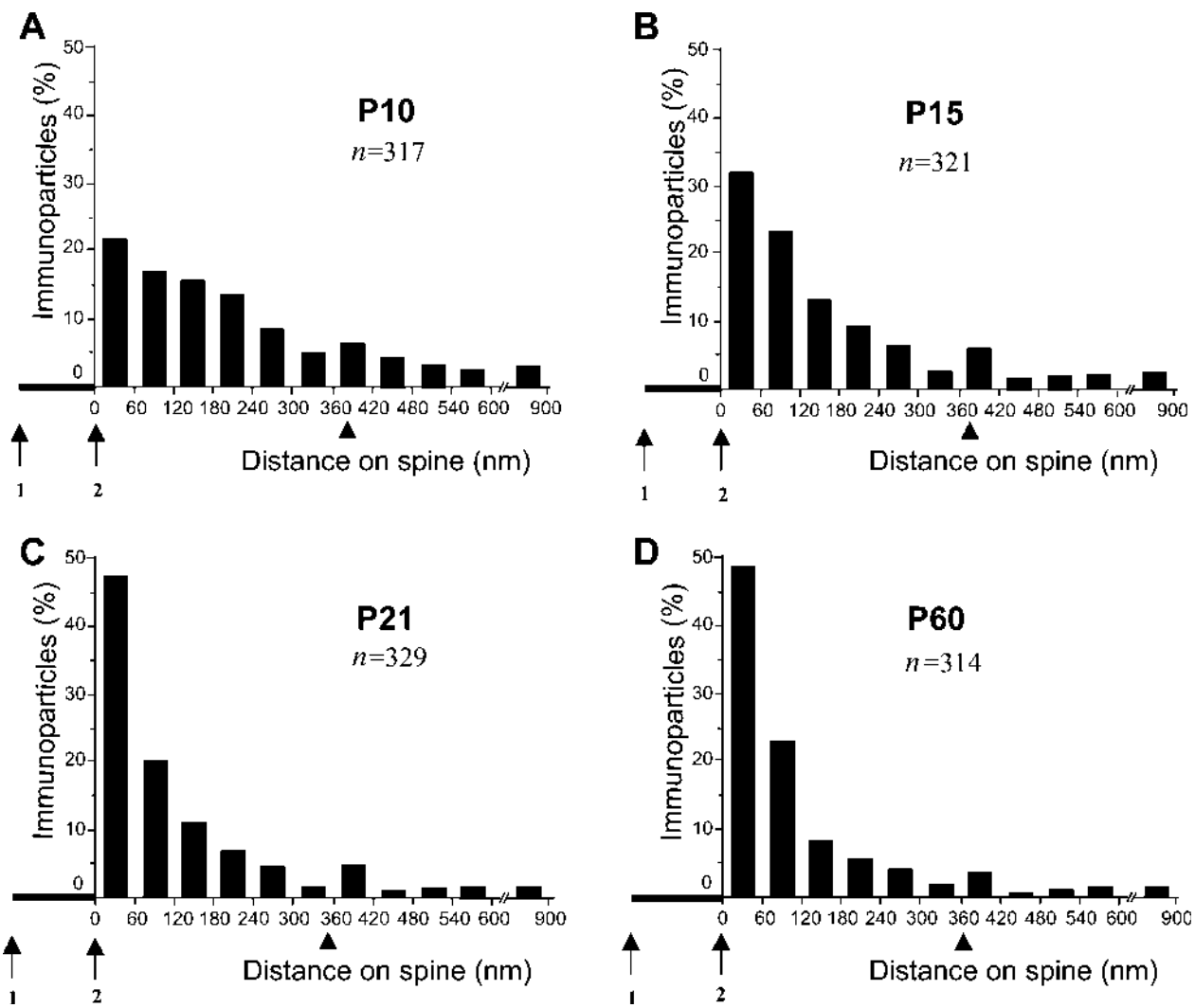


Fig. 9. Distribution of mGluR1α immunoreactivity in relation to PF synapses as assessed by pre-embedding immunogold reactions at P10 (A), P15 (B), P21 (C) and P60 (D). Arrows mark the middle (1) and the edge (2) of the average length of the postsynaptic membrane specialisation at each postnatal age. Arrowheads mark the mean head diameters of PC dendritic spines at each postnatal age. Data are expressed as the proportion of immunoparticles at a given distance from the edge of the synaptic specialisation. Measurements show that mGluR1α was more concentrated in a perisynaptic annulus at P21 and P60 than at younger ages. In contrast, in younger animals, mGluR1α was distributed along a broader membrane segment. At P10 it was more uniformly distributed along the dendritic spine plasma membrane.

mals, were analysed for each postnatal age. Since the distributions in the two samples for each age did not differ from each other (Kolmogorov–Smirnov test, $P > 0.27$, P10; $P > 0.39$, P15; $P > 0.43$, P21; $P > 0.48$, P60), the data were pooled. The mean length of the synaptic membrane specialisation of the immunopositive PCs spines facing PFs at P10, P15, P21 and P60 was 261.49 ± 86.25 nm, 264.37 ± 84.40 nm, 272.93 ± 95.52 nm and 275.48 ± 87.80 nm, respectively, as measured from single sections. The mean head diameters of PC spines were estimated from serial sections at P10, P15, P21 and P60, and they were 369.83 ± 65.67 nm, 366.17 ± 61.42 nm, 355.26 ± 53.58 nm and 359.77 ± 63.53 nm, respectively.

The counts of immunoparticles were normalised to the observed relative frequency of the 60-nm membrane segments at a given distance in the sample spine population. The data expressed in this way showed the change in density of receptor as a function of distance from the PF synapse.

Immunogold particles for mGluR1α were preferentially located in a perisynaptic position (Fig. 9) at each postnatal age studied. However, following normalisation for the membrane area, differences in density along the dendritic spine plasma membrane were detected. At P10, it is apparent that about 25% of all receptor immunoparticles are within 60 nm of the synaptic membrane specialisation (Fig. 9), but receptor density remained relatively uniform in the 300 nm band around the synapse. At P15, mGluR1α became progressively concentrated in a perisynaptic annulus (35%). Furthermore, at P21 and P60, a high density of immunoparticles (about 48%) was concentrated within 60 nm of the synaptic membrane specialisation (Fig. 9). Immunoparticle concentration dropped markedly as a function of distance from the synapse.

The distribution of mGluR1α immunoparticles for each postnatal age was compared pairwise. No differences were found between the distribution of mGluR1α at P21 and P60 ($P > 0.51$). However, differences were detected when the distribution of immunoparticles at P21 and P60 was compared with that at P10 and P15, and when the distribution at P10 was compared to that at P15 ($P < 0.001$ in each case).

DISCUSSION

A major factor affecting the response of a neurone to synaptically released glutamate is the distribution of glutamate receptors along the surface of the neurone. The distribution pattern is established during synaptogenesis and may be dynamically modified during synapse maturation. PCs are good models for studying this pattern because they receive two distinct types of glutamatergic synapses formed by PF and CF which undergo changes in architecture during development (Landis, 1987; Landis et al., 1989) and because they express high levels of mGluR1α, which is involved in synaptic plasticity (Aiba et al., 1994; Shigemoto et al., 1994). The present study provides detailed data on the temporal expression pattern and precise subcellular localisation of mGluR1α in PCs during postnatal development.

Our immunocytochemical results demonstrated that mGluR1α is highly expressed in developing PCs, showing a progressive increase in labelling intensity from E18 to adulthood, parallel to the morphological events occurring during PC ontogenesis (Takács and Hamori, 1994) and suggesting that this receptor is dynamically regulated during postnatal development. Protein expression at E18 is consistent with the detection of the mRNA (Shigemoto et al., 1992). Furthermore, the temporal expression for mGluR1α is in accordance with results obtained by in situ hybridisation (Shigemoto et al., 1992) and binding studies (Catania et al., 1994).

Using high-resolution immunocytochemical techniques and quantification, mGluR1α showed dramatic changes in localisation along the neuronal surface during PC ontogenesis, in association with the arrival and maturation of excitatory inputs. Thus, using immunoperoxidase, mGluR1α was seen concentrated in PC somatic spines facing CFs during the first 2 weeks of development and in PC dendritic spines facing PFs and a few CFs, from the second postnatal week to adulthood. These observations indicate that a major redistribution of receptors occurs in PCs during the first 2 weeks of development and provide evidence that glutamatergic transmission is critical to cerebellar development in vivo.

The use of immunogold methods provided stronger evidence for the association of mGluR1α with PC plasma membranes than that achieved with the immunoperoxidase method. Immunoparticles for mGluR1α were found at the periphery of CF–PC and PF–PC synapses or at more distant sites on the plasma membrane. In addition, the application of quantitative immunocytochemistry demonstrated that mGluR1α has a unique distribution in the plasma membrane of dendritic spines facing PFs. The receptor is concentrated to a different degree in perisynaptic positions, depending on the maturational state of PC-PF synapses. As the PC-PF synapse matures, mGluR1α is redistributed along the plasma membrane and progressively concentrates in perisynaptic sites, which have important functional implications in the acquisition of mature PC responses.

Using the post-embedding immunogold method, mGluR1α was present perisynaptically but absent from the anatomically defined synaptic junction at all postnatal ages. This localisation pattern is similar to that observed previously in adults (Baude et al., 1993; Nusser et al., 1994; Luján et al., 1997) and during postnatal development (Liu et al., 1998; Petralia et al., 1998). In contrast, the AMPA- and delta-type ionotropic glutamate receptors were concentrated in synaptic junctions during development (Petralia et al., 1998; Zhao et al., 1998), suggesting that the segregation of glutamate receptors at individual synapses occurs during early stages of synaptogenesis. Moreover, the location and high density of mGluR1α around the membrane specialisation during development suggests that mGluR1α may also be activated by high frequency presynaptic activity, as demonstrated in the adult cerebellum (Batchelor et al., 1994). This finding brings interesting functional implica-

tions, because the perisynaptic location of mGluR1α means that it is spatially close to the synaptic ionotropic glutamate receptors at all ages. This indicates that since ionotropic glutamate receptors are inserted in the postsynaptic density at early ages, they can be modulated by the mGluR (Pin and Duvoisin, 1995). In addition, the perisynaptic reorganisation of mGluR1α with maturation could mean differences in its efficacy of modulation until mature PC responses are produced.

Developmental regulation of mGluR1α distribution

mGluR1α showed a differential subcellular localisation pattern along the plasma membrane in each postnatal week of PC synaptogenesis (see Fig. 10). During the first week of postnatal development, PC innervation involved the formation of synapses from multiple CFs with somatic spines (Altman and Bayer, 1997). At P0–P3, some CF synapses were already detected, which are presumably functional at this stage (Crépel et al., 1981; Kano et al., 1997). Interestingly, mGluR1α was observed extending uniformly from the PC somata to the stem dendrite or in membrane patches on the cell surface prior to the establishment of CF synapses. Therefore, expression of mGluR1α seems to be independent of the presence of presynaptic terminals (Takács et al., 1997), the receptor being compartmentalised at the subcellular level before the establishment of synaptic contacts. This finding suggests that mGluR1α may be activated by glutamate release either non-synaptically or from neighbouring synapses, and that this mechanism might be involved in synaptogenesis.

The second postnatal week is a period of great developmental activity in PCs. At this time there is considerable outgrowth and differentiation of the PC dendritic arborisation. Thereafter, as dendrites grow, the somatic spines and CF synapses located on them disappear, and the CFs form synaptic contacts on the dendrites (Altman and Bayer, 1997). A few PF synapses begin forming by P7, but the main period of PF synapse formation along the PC dendrite occurs at P10 (Altman and Bayer, 1997). Immunocytochemically, we have demonstrated a progressive reduction in the number of somatic spines from lower to upper portions of PC somata and their final disappearance during this period, coincident with progressive accumulation of mGluR1α in dendritic spines in the molecular layer. Activation of mGluR1α signal transduction pathways during this period may result in elevation of internal Ca^{2+} levels associated with dendritic growth and spine maturation (Casabona et al., 1997).

The third week involves final maturation of excitatory synapses until the adult state is reached, when PCs are innervated by many PFs, but by only one CF (Altman and Bayer, 1997). We have observed that from P21, mGluR1α expression level reached that of the adult and that the receptor was concentrated at dendrites and dendritic spines facing CFs and PFs, respectively. Overall, the qualitative and quantitative changes in mGluR1α observed during these 3 weeks of postnatal

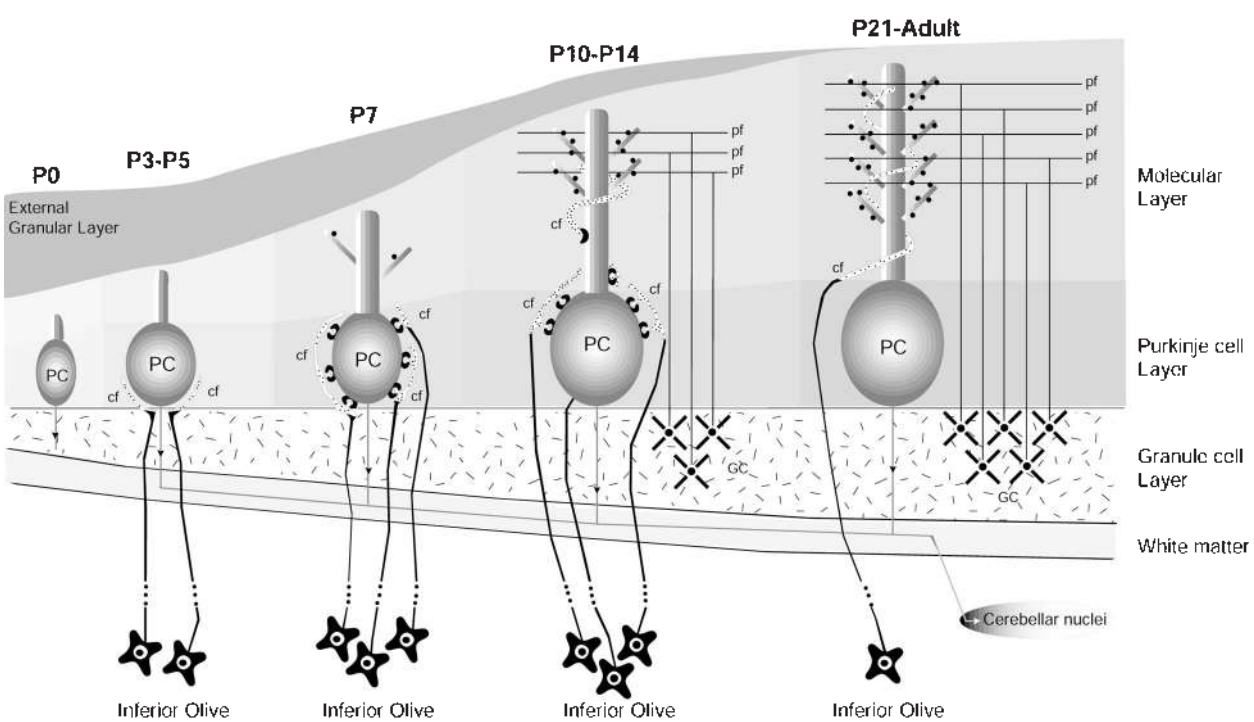


Fig. 10. Postnatal development of mGluR1α in climbing and PFs in the cerebellar cortex. At P0 and P3–P5, mGluR1α was detected uniformly distributed in PCs before the arrival of CFs. CFs innervate PC somata up to the end of the second postnatal week. CF synapses on somatic spines (P7 and P10–P14) contained high levels of mGluR1α. During the second postnatal week, CF synapses disappeared from the somata and were localised in the molecular layer. By P21, CF innervation was reduced to a single fibre per PC. PFs innervate PC dendritic spines from approximately P10 to adulthood. The expression of mGluR1α in PF synapses is very high at all stages. GC, granule cells.

development may alter the excitable properties of PC in the developing cerebellum and modulate the acquisition of mature phenotypic features by PC neurones. Similarly, the localisation of ionotropic glutamate receptors also seems to be developmentally regulated in the cerebellar cortex (Bergmann et al., 1996; Hafidi and Hillman, 1997).

An obvious question suggested by the differential subcellular location of mGluR1α during development is how it is brought about. Whatever the mechanism by which mGluR1α reaches its final destination, receptor sorting presumably involves a selective association with other specific proteins (Brakeman et al., 1997). These proteins may anchor mGluR1α to extrasynaptic and perisynaptic PC membranes. One possibility is that different subcellular compartments have distinct anchoring mechanisms, which could explain why CF synapses are eliminated from the cell body but are maintained on dendrites, providing a potential mechanism for regulating synapse-specific expression of mGluR1α. Further studies are needed to identify the developmental sequence of expression of such anchoring proteins and whether they anchor the same receptor type located at different excitatory synapses.

The role of mGluR1α in the developing cerebellum

The explanation for such a major redistribution of mGluR1α in PCs as development proceeds is not clear, but likely relates to PC plasticity. Combined stimulation of CFs and PFs induces a characteristic long-lasting change in synaptic transmission between PCs and PFs, referred to as long-term depression (LTD; Ito, 1989). The induction of LTD requires the activation of mGluR1 (Daniel et al., 1992; Shigemoto et al., 1994). High concentrations of mGluR1α in PC spines could contribute to the increase on intracellular Ca^{2+} necessary for the induction of LTD (Linden, 1994; Linden and Connor, 1995). This is consistent with results demonstrating that LTD and motor learning are impaired in mice lacking mGluR1 (Aiba et al., 1994; Conquet et al., 1994; Ichise et al., 2000) and could provide information on the process of the establishment of the cerebellar network involved in motor coordination.

mGluRs may also play a role in the early formation of PC synapses. Postsynaptic mechanisms involving mGluR1α during PC synaptogenesis include activation of phospholipase C, producing diacylglycerol, which in turn activates protein kinase C (PKC). The γ isoform of PKC is highly expressed in PCs (Huang et al., 1988; Tanaka and Kondo, 1994). Recent studies demonstrated that in mice lacking mGluR1 or PKCγ, multiple CF innervation persists through adulthood without significant changes in the architecture and function of PF–PC synapses (Kano et al., 1995, 1997; Levenes et al., 1997; Ichise et al., 2000). Therefore, the signal transduction pathway from mGluR1 to PKCγ may play an important role in mediating activities of PF–PC synapses to eliminate multiple CF–PC synapses during postnatal development. Our immunocytochemical results suggest that mGluR1α, the major isoform of mGluR1, may be the subtype involved in such processes. However, innervation of PCs by multiple CFs was recently reported in animals lacking the glutamate receptor δ2 subunit (Kashiwabuchi et al., 1995; Kurihara et al., 1997), indicating that mGluR1α may be necessary but not sufficient for the elimination of redundant synapses.

Previous studies have suggested that the presence of granule cells or functional PF–PC synapses are essential for the regression of multiple CF innervation (Crépel, 1982). Models studied included granule cells destroyed by X-ray-irradiation (Woodward et al., 1974; Crépel and Delhaye-Bouchard, 1979) and mutant mice (*reeler*, *weaver* and *staggerer*) in which granule cells die or PF–PC synapses are impaired (Crépel and Mariani, 1976; Mariani et al., 1977; Crépel et al., 1980; Mariani and Changeux, 1980). Our results show that granule cells express mGluR1α immunoreactivity, albeit at low levels, during development. It is thus possible that mGluR1α expressed in granule cells may be involved in the regression of CFs.

Acknowledgements—We thank Drs. Paul Bolam, Ole Paulsen, Jeff McIlhinney, Alfonso Fairén and Francisco Ciruela for reviewing a previous version of this manuscript and Mrs Alexandra Salewski for the English revision of the manuscript. We also want to thank Dr. Peter Somogyi for offering the facilities of the MRC Anatomical Neuropharmacology Unit to carry out part of this study. This work was supported by a Grant from the European Community (QLG3-CT-1999-00192 to R.L.) and the Spanish Ministry of Education (DGES PM 97-0082 to J.M.J.).

REFERENCES

Abe, T., Sugihara, H., Nawa, H., Shigemoto, R., Mizuno, N., Nakanishi, S., 1992. Molecular characterization of a novel metabotropic glutamate receptor mGluR5 coupled to inositol phosphate/Ca^{2+} signal transduction. J. Biol. Chem. 267, 13361–13368.

Aiba, A., Kano, M., Chen, C., Stanton, M.E., Fox, G.D., Herrup, K., Zwingman, T.A., Tonegawa, S., 1994. Deficient cerebellar long-term depression and impaired motor learning in mGluR1 mutant mice. Cell 79, 377–388.

Altman, J., Bayer, S.A., 1997. Development of the Cerebellar System in Relation to its Evolution, Structure, and Functions. CRC, New York.

Aramori, I., Nakanishi, S., 1992. Signal transduction and pharmacological characteristics of a metabotropic glutamate receptor, mGluR1, in transfected CHO cells. Neuron 8, 757–766.

Baude, A., Nusser, Z., Roberts, J.D.B., Mulvihill, E., McIlhinney, R.A.J., Somogyi, P., 1993. The metabotropic glutamate receptor (mGluR1α) is concentrated at perisynaptic membrane of neuronal subpopulations as detected by immunogold reaction. Neuron 11, 771–787.

Batchelor, A.M., Madge, D.J., Garthwaite, J., 1994. Synaptic activation of metabotropic glutamate receptors in the parallel fibre-Purkinje cell pathway in rat cerebellar slices. Neuroscience 63, 911–915.

Bergmann, M., Fox, P.A., Grabs, D., Post, A., Schilling, K., 1996. Expression and subcellular distribution of glutamate receptor subunits 2/3 in the developing cerebellar cortex. J. Neurosci. Res. 43, 78–86.

Brakeman, P.R., Lanahan, A.A., O'Brien, R., Roche, K., Barnes, C.A., Huganir, R.L., Worley, P.F., 1997. Homer: a protein that selectively binds metabotropic glutamate receptors. Nature 386, 284–288.
Casabona, G., Knopfel, T., Kuhn, R., Gasparini, F., Baumann, P., Sortino, M.A., Copani, A., Nicoletti, F., 1997. Expression and coupling to polyphosphoinositide hydrolysis of group I metabotropic glutamate receptors in early postnatal and adult rat brain. Eur. J. Neurosci. 9, 12–17.
Catania, M.V., Landwehrmeyer, G.B., Testa, C.M., Standaert, D.G., Penney, Jr., J.B., Young, A.B., 1994. Metabotropic glutamate receptors are differentially regulated during development. Neuroscience 61, 481–495.
Conn, P.J., Pin, J.P., 1997. Pharmacology and functions of metabotropic glutamate receptors. Annu. Rev. Pharmacol. Toxicol. 37, 205–237.
Conquet, F., Bashir, Z.I., Davies, C.H., Daniel, H., Ferraguti, F., Bordi, F., Franz-Bacon, K., Reggiani, A., Matarase, V., Conde, F., Collingridge, G.L., Crepel, F., 1994. Motor deficit and impairment of synaptic plasticity in mice lacking mGluR1. Nature 372, 237–243.
Crépel, F., 1982. Regression of functional synapses in the mature mammalian cerebellum. Trends Neuroci. 5, 266–269.
Crépel, F., Mariani, J., 1976. Multiple innervation of Purkinje cells by climbing fibres in the cerebellum of the *weaver* mutant mouse. J. Neurobiol. 7, 579–582.
Crépel, F., Delhaye-Bouchard, N., 1979. Distribution of climbing fibres on cerebellar Purkinje cells in X-irradiated rats: an electrophysiological study. J. Physiol. 290, 97–112.
Crépel, F., Delhaye-Bouchard, N., Gustavino, J.M., Sampaio, I., 1980. Multiple innervation of cerebellar Purkinje cells by climbing fibres in *staggerer* mutant mouse. Nature 283, 483–484.
Crépel, F., Delhaye-Bouchard, N., Dupont, J.L., 1981. Fate of the multiple innvervation of the cerebellar Purkinje cells by climbing fibres in immature control, x-irradiated and hypothyroid rats. Dev. Brain Res. 1, 59–71.
Daniel, H., Hemart, N., Jaillard, D., Crépel, F., 1992. Coactivation of metabotropic glutamate receptors and of voltage-gated calcium channels induces long-term depression in cerebellar Purkinje cells *in vitro*. Exp. Brain Res. 90, 327–331.
Hafidi, A., Hillman, D.E., 1997. Distribution of glutamate receptors GluR2/3 and NR1 in the developing rat cerebellum. Neuroscience 81, 427–436.
Huang, F.L., Yoshida, Y., Nakabayashi, H., Young, W.S., Huang, K.-P., 1988. Immunocytochemical localisation of protein kinase C isozymes in rat brain. J. Neurosci. 8, 4734–4744.
Ichise, T., Kano, M., Hashimoto, K., Yanagihara, D., Nakao, K., Shigemoto, R., Katsuki, M., Aiba, A., 2000. mGluR1 in cerebellar Purkinje cells essential for long-term depression, synapse elimination, and motor coordination. Science 288, 1832–1835.
Ito, M., 1984. The Cerebellum and Neuronal Control. Raven, New York.
Ito, M., 1989. Long-term depression. Annu. Rev. Neurosci. 12, 85–102.
Jaarsma, D., Dino, M.R., Ohishi, H., Shigemoto, R., Mugnaini, E., 1998. Metabotropic glutamate receptors are associated with non-synaptic appendages of unipolar brush cells in rat cerebellar cortex and cochlear nuclear complex. J. Neurocytol. 27, 303–327.
Kano, M., Hashimoto, K., Chen, C., Abeliovich, A., Aiba, A., Kurihara, H., Watanabe, M., Inoue, Y., Tonegawa, S., 1995. Impaired synapse elimination during cerebellar development in PKCγ mutant mice. Cell 83, 1223–1231.
Kano, M., Hashimoto, K., Kurihara, H., Watanabe, M., Inoue, Y., Aiba, A., Tonegawa, S., 1997. Persistent multiple climbing fibre innervation of cerebellar Purkinje cells in mice lacking mGluR1. Neuron 18, 71–79.
Kashiwabuchi, N., Ikeda, K., Araki, K., Hirano, T., Shibuki, K., Takayama, C., Inoue, Y., Kutsuwada, T., Yagi, T., Kang, Y., Aizawa, S., Mishina, M., 1995. Impairment of motor coordination, Purkinje cell synapse formation, and cerebellar long-term depression in GluRδ2 mutant mice. Cell 81, 245–252.
Kurihara, H., Hashimoto, K., Kano, M., Takayama, C., Sakimura, K., Mishina, M., Inoue, Y., Watanabe, M., 1997. Impaired parallel fibre-Purkinje cell synapse stabilisation during cerebellar development of mutant mice lacking the glutamate receptor δ2 subunit. J. Neurosci. 17, 9613–9623.
Landis, M.D., 1987. Initial junctions between developing parallel fibers and Purkinje cells are different from mature synaptic junctions. J. Comp. Neurol. 260, 513–525.
Landis, M.D., Payne, H.R., Weinstein, L.A., 1989. Changes in the structure of synaptic junctions during climbing fiber synaptogenesis. Synapse 4, 281–293.
Levenes, C., Daniel, H., Jaillard, D., Conquet, F., Crépel, F., 1997. Incomplete regression of multiple climbing fibre innervation of cerebellar Purkinje cells in mGluR1 mutant mice. NeuroReport 8, 571–574.
Linden, D.J., 1994. Long-term depression in the mammalian brain. Neuron 12, 457–472.
Linden, D.J., Connor, J.A., 1995. Long-term synaptic depression. Annu. Rev. Neurosci. 18, 319–357.
Liu, X.B., Muñoz, A., Jones, E.G., 1998. Changes in subcellular localisation of metabotropic glutamate receptor subtypes during postnatal development of mouse thalamus. J. Comp. Neurol. 395, 450–465.
Luján, R., Nusser, Z., Roberts, J.D.B., Shigemoto, R., Somogyi, P., 1996. Perisynaptic location of metabotropic glutamate receptors mGluR1 and mGluR5 on dendrites and dendritic spines in the rat hippocampus. Eur. J. Neurosci. 8, 1488–1500.
Luján, R., Roberts, J.D.B., Shigemoto, R., Ohishi, H., Somogyi, P., 1997. Differential plasma membrane distribution of metabotropic glutamate receptors mGluR1α, mGluR2 and mGluR5, relative to neurotransmitter release sites. J. Chem. Neuroanat. 13, 219–241.
Mariani, J., Changeux, J.P., 1980. Multiple innervation of Purkinje cells by climbing fibres in the cerebellum of the adult *staggerer* mutant mouse. J. Neurobiol. 11, 41–50.
Mariani, J., Crépel, F., Mikoshiba, K., Changeux, J.P., Sotelo, C., 1977. Anatomical, physiological and biochemical studies of the cerebellum from the *reeler* mutant mouse. Phil. Trans. R. Soc. Lond. 281, 1–28.
Martin, L.J., Backstone, C.D., Huganir, R.L., Price, D.L., 1992. Cellular localization of a metabotropic glutamate receptor in rat brain. Neuron 9, 259–270.
Masu, M., Tanabe, Y., Tsuchida, K., Shigemoto, R., Nakanishi, S., 1991. Sequence and expression of a metabotropic glutamate receptor. Nature 349, 760–765.
Nakanishi, S., 1994. Metabotropic glutamate receptors: synaptic transmission, modulation, and plasticity. Neuron 13, 1031–1037.
Nusser, Z., Mulvihill, E., Streit, P., Somogyi, P., 1994. Subsynaptic segregation of metabotropic glutamate receptors as revealed by immunogold localisation. Neuroscience 61, 421–427.
Nusser, Z., Somogyi, P., 1997. Compartmentalised distribution of GABAA and glutamate receptors in relation to transmitter release sites on the surface of cerebellar neurones. Prog. Brain Res. 114, 109–127.
Palay, S., Chan-Palay, V., 1974. Cerebellar cortex: Cytology and Organisation. Springer, New York.
Petralia, R.S., Zhao, H.-M., Wang, Y.-X., Wenthold, R.J., 1998. Variations in the tangential distribution of postsynaptic glutamate receptors in Purkinje cell parallel and climbing fibre synapses during development. Neuropharmacology 37, 1321–1334.
Pin, J.P., Duvoisin, R., 1995. The metabotropic glutamate receptors: structure and function. Neuropharmacology 34, 1–26.
Ryo, Y., Miyawaki, A., Furuichi, T., Mikoshiba, K., 1993. Expression of the metabotropic glutamate receptor mGluR1a and the ionotropic glutamate receptor GluR1 in the brain during the postnatal development of normal mouse and in the cerebellum from mutant mice. J. Neurosci. Res. 36, 19–32.

Shigemoto, R., Nakanishi, S., Mizuno, N., 1992. Distribution of mRNA for a metabotropic glutamate receptor (mGluR1) in the central nervous system: an *in situ* hybridisation in adult and developing rat. J. Comp. Neurol. 322, 121–135.

Shigemoto, R., Abe, T., Nomura, S., Nakanishi, S., Hirano, T., 1994. Antibodies inactivating mGluR1 metabotropic glutamate receptor block long-term depression in cultured Purkinje cells. Neuron 12, 1245–1255.

Sotelo, C., 1978. Purkinje cell ontogeny: formation and maintenance of spines. Prog. Brain Res. 48, 149–170.

Takács, J., Hamori, J., 1994. Developmental dynamics of Purkinje cells and dendritic spines in rat cerebellar cortex. J. Neurosci. Res. 38, 515–530.

Takács, J., Gombos, G., Gorcs, T., Becker, T., de Barry, J., Hámori, J., 1997. Distribution of metabotropic glutamate receptor type 1a in Purkinje cell dendritic spines is independent of the presence of presynaptic parallel fibres. J. Neurosci. Res. 50, 433–442.

Tanaka, O., Kondo, H., 1994. Localisation of mRNAs from three novel members (β3, β4 and γ2) of phospholipase C family in mature rat brain. Neurosci. Lett. 182, 17–20.

Woodward, D.J., Hoffer, B.J., Altman, J., 1974. Physiological and pharmacological properties of Purkinje cells in rat cerebellum degranulated by postnatal x-irradiation. J. Neurobiol. 5, 283–304.

Zhao, H.-M., Wenthold, R.J., Petralia, R.S., 1998. Glutamate receptor targeting to synaptic populations on Purkinje cells is developmentally regulated. J. Neurosci. 18, 5517–5528.

(*Accepted* 18 *April* 2001)